# Lawrence Berkeley National Laboratory

## Lawrence Berkeley National Laboratory

### Title

Stimulated Terahertz Emission from Intra-Excitonic Transitions in Cu2O

### Permalink

https://escholarship.org/uc/item/9w52w3h0

### Authors

Huber, Rupert
Schmid, Ben A.
Shen, Y. Ron
et al.

### Publication Date

2005-06-16

eScholarship.org Powered by the California Digital Library
University of California

# Stimulated Terahertz Emission from Intra-Excitonic Transitions in $Cu_2O$

Rupert Huber, Ben A. Schmid, Y. Ron Shen, Daniel S. Chemla, and Robert A. Kaindl
*Department of Physics, University of California at Berkeley, and Material Sciences Division, E.O. Lawrence Berkeley National Laboratory, Berkeley, California 94720, USA*

We report the first observation of stimulated emission of terahertz radiation from internal transitions of excitons. The far-infrared electromagnetic response of $Cu_2O$ is monitored via broadband terahertz pulses after ultrafast resonant excitation of three-dimensional $3p$ excitons. Stimulated emission from the $3p$ to the energetically lower $2s$ bound level occurs at a photon energy of 6.6 meV, with a cross section of $\sim 10^{-14}\mathrm{cm}^2$. Simultaneous excitation of both exciton levels, in turn, drives quantum beats which lead to efficient terahertz emission sharply peaked at the difference frequency.

PACS numbers: 71.35.-y, 78.47.+p, 42.65.-k

The concept of excitons has been exceptionally successful in describing the complex many-body problem of a photoexcited semiconductor in the dilute limit [1, 2]. These quasi-particles can effectively be described as a hydrogen-like entity of an electron bound to a hole via the long-range Coulomb interaction. Thus, excitons are analogous to bound states in many other physical systems such as atoms or nuclei. These aspects have motivated the search for macroscopically ordered states and Bose-Einstein condensation also in excitons [3, 4]. Cuprous oxide ($Cu_2O$) is a semiconductor that hosts a uniquely well-defined Rydberg series of bound excitonic states with sharp visible absorption lines and is one of the most promising candidates in this field [5, 6].

Most of the spectroscopic information on excitons has been extracted from optical techniques probing interband transitions. However, such experiments provide only indirect access to the internal structure. A most direct approach to investigate intra-excitonic absorption requires studies in the mid to far infrared spectral domain [6–8]. In recent years various sources for terahertz (THz) radiation have been developed [9]. THz spectroscopy has evolved as a powerful tool for probing low-energy excitations in semiconductors with ultrafast temporal resolution [7, 10, 11]. Recently, absorption of THz radiation promoting ground state excitons into higher bound energy levels was used to explore exciton formation dynamics on a picosecond timescale [7].

Theoretical studies suggest how the underlying elementary quantum processes could be effectively reversed to induce terahertz gain from inverted exciton populations [12, 13]. Stimulated emission of electromagnetic radiation constitutes a fundamental process in physics, but – to the best of our knowledge – it has not yet been observed between internal exciton levels.

In this Letter, we report the first direct observation of stimulated emission of terahertz radiation from intra-excitonic transitions. After resonant photoexcitation of $3p$ excitons in the semiconductor $Cu_2O$ we use broadband THz pulses to induce internal dipole transitions to the 2s state. This process manifests itself via a negative change of the absorption coefficient at the resonant photon energy of 6.6 meV. Incoherent population inversion and coherent resonant Raman scattering both contribute to this effect. Furthermore, we demonstrate a novel scheme for resonant THz generation via beating of the $3p$ and $2s$ states simultaneously excited by visible light pulses.

All experiments are performed at low temperature ($T = 6$ K) in a 330-$\mu$m-thick, naturally grown high-quality $Cu_2O$ crystal. The visible absorption spectrum, shown in Fig. 1, is dominated by a series of sharp lines originating from the $2p$, $3p$, $4p$, and $5p$ excitons (yellow series), followed by the continuum of unbound states. Owing to the positive parity of the valence and conduction band minima at the Brillouin zone center, even parity $s$- and $d$-excitons are dipole forbidden [14]. Fig. 1 shows a detailed exciton term scheme, with the energy difference to the $3p$ level given on the left. Far infrared transmission measurements confirm the unexcited sam-

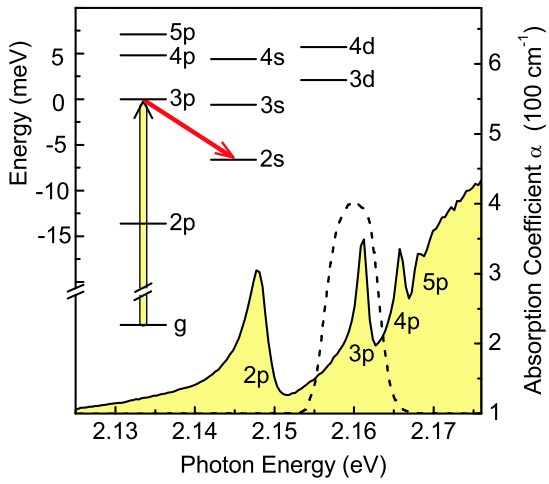


FIG. 1: (color online). Optical absorption spectrum of the $Cu_2O$ crystal studied in this work, at $T = 6$ K. Exciton absorption lines exhibit widths of 3.6 meV ($2p$) and 1.8 meV ($3p$). The term scheme indicates the yellow exciton series, with energy differences given with respect to the $3p$ exciton level [14]. Resonant excitation of $3p$ excitons is indicated by the thick upward arrow (a corresponding typical pump spectrum is shown by the dashed curve). Internal exciton transitions from $p$- to $s$- or $d$-states are dipole allowed (solid arrow).

ple to be transparent with no absorption features in the window between 1 and 12 meV.

Our experimental scheme is based on an ultrafast regenerative Ti:sapphire amplifier operating at 250-kHz repetition rate, which delivers 42-fs light pulses at a center wavelength of 800 nm. Nearly bandwidth-limited light pulses tunable around 575 nm wavelength are obtained by subsequent optical parametric amplification. We use a grating-based pulse shaper to tailor the energy and width of these visible pulses, in order to selectively photoexcite specific bound exciton states or the continuum of unbound electron-hole ($e$-$h$) pairs. A resulting typical pump spectrum is indicated by the dashed curve in Fig. 1. Ultrashort THz probe pulses are obtained by optical rectification of a second branch of the near-infrared laser output in a 500-$\mu$m-thick ZnTe crystal. The real-time electric field trace $E_{\mathrm{THz}}(t)$ of the transmitted THz pulse is recorded by means of electro-optic sampling with a large signal-to-noise ratio of $10^5$. Owing to THz field measurement directly in the time-domain, both real and imaginary parts of the optical response are obtained on equal footing.

In a first set of experiments, we resonantly excite the $Cu_2O$ sample at specific exciton absorption lines and follow the subsequent transient changes in the far-infrared response via a time-delayed THz pulse. Figures 2(a)-(c) show the transmitted THz field $E_{\mathrm{THz}}(t)$ without photoexcitation (thin lines, downscaled by a factor of 500), and its transient change $\Delta E_{\mathrm{THz}}(\Delta t, t)$ (thick lines) induced by photoexcitation at three characteristic wavelengths. The temporal delay between the yellow pump pulse and the electro-optic gating pulse is kept fixed at $\Delta t = 1$ ps. Differential transmission spectra $\Delta T/T$ corresponding to each case are shown in the right panels of Fig. 2. The response reveals a critical wavelength dependence: excitation in the continuum [Figs. 2(a),(d)] or at the $2p$ resonance [Figs. 2(c),(f)] induces electric field transients that resemble the reference pulse with a phase offset. A featureless broadband decrease of transmission results. In contrast, resonant excitation of $3p$ excitons shows a very different shape of the induced field and a strongly structured transmission change [Figs. 2(b),(e)]. In particular, we find a remarkable increased transmission around 6.6 meV photon energy.

We now use the full knowledge of the THz electric fields in both amplitude and phase to determine directly the change of the complex refractive index $\tilde{n}(\omega) \equiv n(\omega) + i\frac{c}{2\omega}\alpha(\omega)$, where $n$ denotes the real part of the refractive index and $\alpha$ is the absorption coefficient. Since the excitation density decays exponentially along the propagation length $z$ inside the crystal, we express the locally induced change as $\Delta\tilde{n}(z,\omega) = \Delta\tilde{n}(\omega)\ \exp\{-\alpha_{\mathrm{vis}} z\}$. Here, $\alpha_{\mathrm{vis}}$ is the absorption coefficient in the visible (Fig. 1) and $\Delta\tilde{n}(\omega)$ refers to the pump-induced change at the entrance face of the crystal. Based on this information and including the known refractive index of $Cu_2O$ [15], the complex transfer function of the photo-excited sample may be calculated via the well-established Fresnel matrix formalism. In turn, we directly obtain the induced change of the refractive index and absorption at each frequency by varying $\Delta\tilde{n}(\omega)$ and fitting the resulting response function to the experimental data. All relevant results discussed in the following are insensitive to the exact parameters used in the analysis.

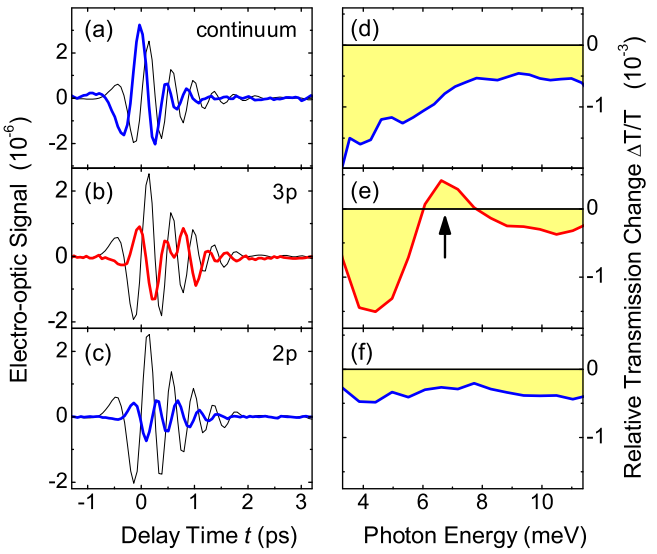


FIG. 2: (color online). (a)-(c) Pump-induced changes $\Delta E_{\mathrm{THz}}$ (thick lines) at $\Delta t = 1$ ps after excitation, and reference THz fields $E_{\mathrm{THz}}$ (thin lines) without excitation. The reference fields are downscaled by a factor of 500 for better visibility. Pump spectra are centered (a) in the continuum at 2.206 eV, (b) at the yellow $3p$ exciton line, and (c) at the $2p$ exciton line. (d)-(f) Corresponding relative transmission changes $\Delta T/T$. Arrow: enhanced transmission at 6.6 meV.

Figure 3 displays the differential changes $\Delta n$ and $\Delta\alpha$ obtained from the traces in Fig. 2. Continuum excitation [topmost curves in Figs. 3(a),(b)] results in a predominantly inductive THz response, well explained by the Drude theory (dashed-dotted lines) of a conducting $e$-$h$ gas. In contrast, resonant $2p$ excitation induces only small changes in the refractive index (lowest curves in Fig. 3) as expected for insulating, bound states. The most striking response is obtained after selective excitation of the $3p$ interband resonance, yielding a pronounced spectral structure in both $\Delta\alpha$ and $\Delta n$. With increasing frequency, a peak of enhanced absorption occurs at 4.5 meV, followed by a narrow minimum of $\Delta\alpha$ at 6.6 meV. Indeed, here the induced absorption becomes negative. We emphasize three key aspects of this observation: ($i$) unexcited $Cu_2O$ shows no discernible THz absorption in this frequency range, ($ii$) the minimum with $\Delta\alpha < 0$ appears exclusively after resonant excitation of $3p$ excitons, and ($iii$) the observed resonance energy of 6.6 meV is precisely identical with the $3p$–$2s$ level spacing (Fig. 1). Hence, we can identify the negative absorption peak as stimulated emission of THz radiation via the $3p \rightarrow 2s$ intra-excitonic transition.

For further analysis, we model the lineshape of the THz

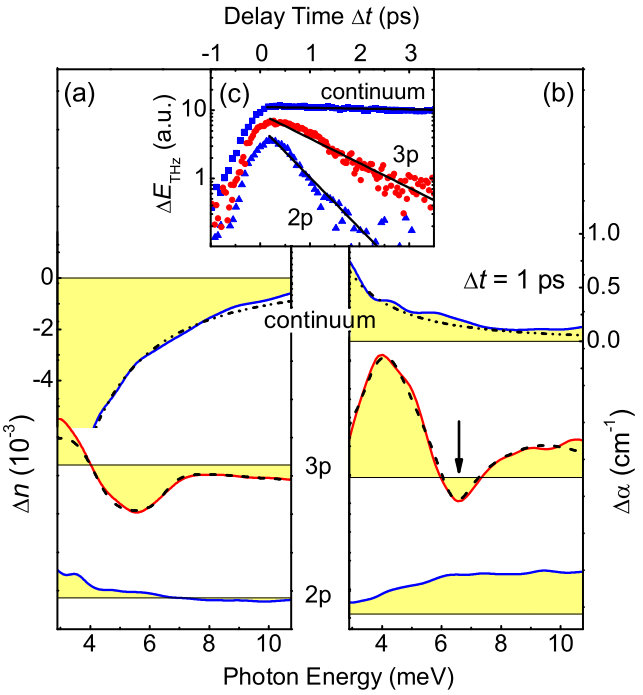


FIG. 3: (color online). THz response at $\Delta t = 1$ ps after excitation of $2p$ or $3p$ excitons, or the continuum. (a),(b) Changes of refractive index $\Delta n$ and absorption $\Delta\alpha$ (solid lines, offset vertically for clarity). Dash-dotted lines: a Drude response (topmost curves) with screened plasmon energy $\hbar\omega_{\rm pl} = 0.3$ meV and damping $\Gamma/2\pi = 0.4$ meV. Dashed lines: model of three oscillators (lower curves) with energies (and linewidths) $E_1 = 4.5$ meV (2.5 meV), $E_2 = 6.6$ meV (1.6 meV), and $E_3 = 9.5$ meV (4 meV), and relative oscillator strengths as given in the text. The vertical arrow marks the negative absorption change occurring around 6.6 meV. (c) Ultrafast pump-probe dynamics of the induced change of the THz field at corresponding pump energies.

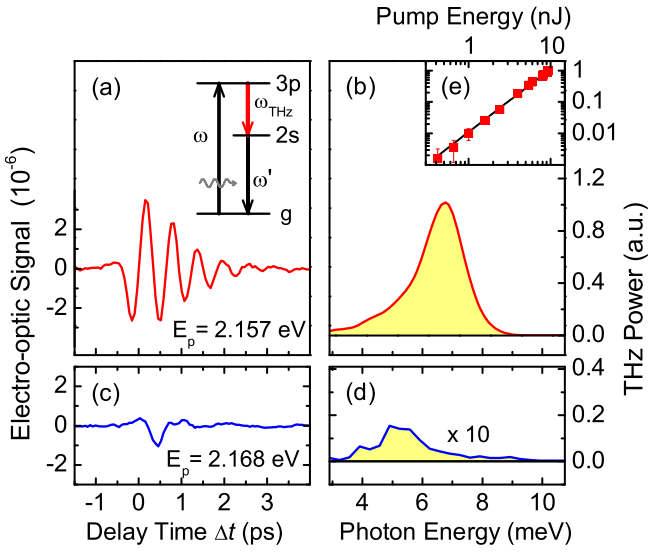


FIG. 4: (color online). THz generation in $Cu_2O$: (a) Real time trace and (b) normalized power spectrum of THz pulses (FWHM: 1.7 meV) obtained with the pump centered at 2.157 eV (close to the $3p$ resonance). The spectral width of the pump pulse is 12 meV (FWHM). Inset: term scheme of the underlying quantum process. (c),(d) THz emission for pump centered at 2.168 eV. (e) The emitted THz power for excitation at 2.157 eV scales quadratically as a function of the pump pulse energy.

response upon $3p$ excitation. A faithful representation of the experiment is achieved with a model of three oscillators (dashed lines, Fig. 3). By comparison with the term scheme of Fig. 1, we attribute the lowest-frequency oscillator centered at 4.5 meV to the joint effects of $3p \rightarrow 4s$ and $3p \rightarrow 4d$ transitions. The center oscillator at 6.6 meV exhibits a negative oscillator strength, in accordance with the $3p \rightarrow 2s$ stimulated emission. Finally, a component at 9.5 meV phenomenologically describes all transitions to higher bound states. The relative oscillator strengths $f_1$:$f_2$:$f_3$ = 2.7:(-1):1.1 agree qualitatively with a hydrogen model [4.4:(-1):2], thus supporting this assignment [16]. A more rigorous theory should also take into account the partial d-character of the 2s exciton in $Cu_2O$, as described in Ref. 14. With an estimated density of $3p$ excitons of $3 \times 10^{13}$ cm$^{-3}$ we obtain a cross section for the $3p \rightarrow 2s$ transition of $\sigma \approx 10^{-14}$ cm$^2$. This value compares well with order-of-magnitude estimates based on hydrogenic exciton wavefunctions [12].

It should be noted that the THz emission may be sensitive to two types of excitations [13, 17]: (*i*) *coherent excitonic polarizations,* where THz emission results from stimulated Raman scattering as a single-step nonlinear optical process: the THz field coherently couples polarizations from the $3p$ to the $2s$ state, from which in turn visible pump photons are scattered into the THz field. (*ii*) *incoherent exciton populations,* where stimulated emission is driven purely by population inversion and subsequent hot luminescence, analogous to atomic lasers. The relative importance of these processes depends on the polarization and population decay times. A dephasing time for the $3p$ level can be estimated from the visible linewidth, which yields $T_2 \approx 0.7$ ps assuming predominantly homogeneous broadening for our high-quality $Cu_2O$ crystal. Population relaxation can be deduced from the dynamics of the induced THz response. Fig. 3(c) depicts an increasingly faster exponential decay as we turn from continuum states ($\tau = 36$ ps), via the 3p ($\tau = 1.3$ ps) to the $2p$ exciton ($\tau = 0.8$ ps). The relative spectral shape does not vary strongly in time (not shown). The relaxation is explained by recombination and scattering into $1s$ excitons mediated by optical phonon interactions [18]. On this basis, stimulated THz emission after $3p$ excitation occurs both during an initial regime of coherent excitonic polarizations and from the subsequent incoherent inverted population.

In the following, we show that coherent manipulation of the $3p \rightarrow 2s$ transition may be exploited to emit THz radiation even without stimulation by external THz fields. For this second set of experiments, the pump spec-

trum is tuned to simultaneously overlap both the $3p$ and the dipole-forbidden $2s$ resonances. No THz probe light is incident on the sample. We observe emission of a coherent THz field shown in Fig. 4(a). The transient is detected electro-optically by scanning the delay $\Delta t$ between the visible pump and the gating pulse. The corresponding power spectrum in Fig. 4(b) peaks at 6.6 meV and exhibits a width of 1.7 meV (FWHM). This lineshape coincides with the values deduced from the $3p \rightarrow 2s$ transition in Fig. 3, corroborating that the THz transient originates from the same internal exciton transition. The absolute size of these emitted fields is comparable to the transients $\Delta E_{\mathrm{THz}}$ in Fig. 2 stimulated by a far-infrared seed pulse. This fact implies that the generation mechanism cannot be explained by a spontaneous version of the emission process discussed above. Moreover, we find that the THz polarization is parallel to the linear polarization of the pump light. In contrast, the polarization of the stimulated change $\Delta E_{\mathrm{THz}}$, described further above, is determined by the probe pulses.

We interpret this THz emission as resulting from quantum beats between coherent exciton polarizations. Visible light induces $3p$ exciton polarizations, while the low-energy wing of the pump spectrum couples the $2s$ level to the ground state, e.g. via a weak quadrupole or surface field assisted dipole transition [12, 19]. As $3p$ and $2s$ states feature opposite parity, quantum beats between them act as a radiating dipole. The THz generation may be expressed as an effective difference frequency process, described by the nonlinear susceptibility [20]

$$\chi^{(2)}_{\mathrm{eff}} \propto \frac{\mathrm{M}_{3p}\mathrm{M}_{2s}\mathrm{M}_{3p-2s}}{(\omega - \omega_{3p} + i\Gamma_{3p})(\omega_{\mathrm{THz}} - \omega_{3p-2s} + i\Gamma_{3p-2s})} \ ,$$

where $\mathrm{M}_{3p}$ and $\mathrm{M}_{2s}$ are the visible interband matrix elements and $\mathrm{M}_{3p-2s}$ is the THz dipole matrix element. Furthermore, $\omega$ and $\omega_{\mathrm{THz}}$ are the frequencies of visible pump and emitted THz fields, and $\omega_{3p}$ and $\omega_{3p-2s}$ are visible $3p$ and THz $3p \rightarrow 2s$ resonance energies with corresponding dephasing constants $\Gamma_i$. The three-wave interaction is schematically indicated in Fig. 4(a). In our experiment both terms in the denominator become resonant, which leads to a high nonlinearity despite the relative weakness of the coupling between 2s excitons and the ground state. Off-resonant pumping reduces the conversion efficiency dramatically [Figs. 4(c),(d)]. As shown in Fig. 4(e), the emitted THz intensity scales quadratically with the pump power which further supports this $\chi^{(2)}$ picture. From the pulse intensities and effective interaction length we estimate a nonlinearity of $\chi^{(2)}_{\mathrm{eff}} \gtrsim 10$ pm/V. This value exceeds the high background nonlinearity of non-centrosymmetric materials such as ZnTe, which is widely used for THz generation [21].

In conclusion, we report the first direct observation of stimulated emission of electromagnetic radiation from internal transitions of excitons. Furthermore, we demonstrate that such atomic-like transitions in $Cu_2O$ may also be employed for efficient THz generation via a doubly resonantly enhanced nonlinearity. While the measured stimulated emission is still too weak to give rise to overall THz gain, the scheme is upscalable. Because of the rather large absorption length of $\sim$ 30 $\mu$m for visible light in $Cu_2O$, the excitation densities reached in our setup are several orders of magnitude below the excitonic Mott density. Thus, higher pump energies make this approach potentially interesting for efficient amplification of THz radiation. Similar experiments may now also become possible in custom-tailored semiconductor nanostructures opening up entirely new perspectives.

We thank N. C. Nielsen for valuable discussions. This work was supported by the Director, Office of Science, Basic Energy Sciences, U.S. Department of Energy, under contract DE-AC02-05CH11231. R. H. acknowledges support from the Alexander von Humboldt foundation.

[1] E. I. Rashba, *Excitons* (North-Holland, Amsterdam, 1982).
[2] H. Haug and S. W. Koch, *Quantum Theory of the Optical and Electronic Properties of Semiconductors* (World Scientific, Singapore, 2004).
[3] L. V. Keldysh and A. N. Kozlov, Sov. Phys. JETP **27**, 521 (1968).
[4] L. V. Butov *et al.*, Nature **417**, 47 (2002).
[5] D. W. Snoke *et al.*, Phys. Rev. Lett. **64**, 2543 (1990); K. E. O'Hara and J. P. Wolfe, Phys. Rev. B **62**, 12909 (2000).
[6] M. Kubouchi *et al.*, Phys. Rev. Lett. **94**, 016403 (2005).
[7] R. A. Kaindl *et al.*, Nature **423**, 734 (2003).
[8] M. Jörger *et al.*, phys. stat. sol. (b) **238**, 470 (2003).
[9] for a review see e.g. B. Ferguson and X.-C. Zhang, Nat. Mat. **1**, 26 (2002) and references therein.
[10] R. Huber *et al.*, Nature **414**, 286 (2001); R. Huber *et al.*, Phys. Rev. Lett. **94**, 027401 (2005).
[11] C. W. Luo *et al.*, Phys. Rev. Lett. **92**, 047402 (2004).
[12] S. Nikitine, J. Phys. Chem. Solids **45**, 949 (1984).
[13] M. Kira and S. W. Koch, Phys. Rev. Lett. **93**, 076402 (2004).
[14] C. Uihlein *et al.*, Phys. Rev. B **23**, 2731 (1981).
[15] Landoldt-Börnstein, *Cuprous oxide ($Cu_2O$) optical properties*, Group III Condensed Matter, Subvolume C (Springer, Berlin, 1998).
[16] H. A. Bethe and E. E. Salpeter, *Quantum Mechanics of One- and Two-Electron Atoms*, Academic Press, New York (1957).
[17] Y. R. Shen, Phys. Rev. B **14**, 1772 (1976).
[18] P. Y. Yu and Y. R. Shen, Phys. Rev. B **17**, 4017 (1978).
[19] S. Lien Chuang *et al.*, Phys. Rev. Lett. **68**, 102 (1992).
[20] The relation follows from a simplified treatment of stimulated polariton scattering as discussed in Y. R. Shen, *The Principles of Nonlinear Optics* (Wiley, New York, 2002).

[21] Q. Wu and X.-C. Zhang, Appl. Phys. Lett. **68**, 1604 (1996).